THE JOURNAL OF BIOLOGICAL CHEMISTRY VOL. 285, NO. 51, pp. 40373–40386, December 17, 2010

Ligand- and Subunit-specific Conformational Changes in the Ligand-binding Domain and the TM2-TM3 Linker of $\alpha1\ \beta2\ \gamma2$ $GABA_A$ Receptors*

Received for publication, July 5, 2010, and in revised form, October 4, 2010 Published, JBC Papers in Press, October 11, 2010, DOI 10.1074/jbc.M110.161513

Qian Wang[1], **Stephan A. Pless**[2], **and Joseph W. Lynch**[3]

From the Queensland Brain Institute and School of Biomedical Sciences, University of Queensland, Brisbane, Queensland 4072, Australia

Cys-loop receptor ligand binding sites are located at subunit interfaces where they are lined by loops A–C from one subunit and loops D–F from the adjacent subunit. Agonist binding induces large conformational changes in loops C and F. However, it is controversial as to whether these conformational changes are essential for gating. Here we used voltage clamp fluorometry to investigate the roles of loops C and F in gating the $\alpha1\ \beta2\ \gamma2$ $GABA_A$ receptor. Voltage clamp fluorometry involves labeling introduced cysteines with environmentally sensitive fluorophores and inferring structural rearrangements from ligand-induced fluorescence changes. Previous attempts to define the roles of loops C and F using this technique have focused on homomeric Cys-loop receptors. However, the problem with studying homomeric receptors is that it is difficult to eliminate the possibility of bound ligands interacting directly with attached fluorophores at the same site. Here we show that ligands binding to the $\beta2$-$\alpha1$ interface GABA binding site produce conformational changes at the adjacent subunit interface. This is most likely due to agonist-induced loop C closure directly altering loop F conformation at the adjacent $\alpha1$-$\beta2$ subunit interface. However, as antagonists and agonists produce identical $\alpha1$ subunit loop F conformational changes, these conformational changes appear unimportant for gating. Finally, we demonstrate that TM2-TM3 loops from adjacent $\beta2$ subunits in $\alpha1\ \beta2$ receptors can dimerize via K24′C disulfides in the closed state. This result implies unexpected conformational mobility in this crucial part of the gating machinery. Together, this information provides new insights into the activation mechanisms of Cys-loop receptors.

$GABA_A$ receptor ($GABA_AR$)[4] chloride channels are pentameric Cys-loop receptors that mediate most of the fast inhibitory synaptic transmission in the brain (1). This family also includes nicotinic acetylcholine receptors (nAChRs), glycine receptors (GlyRs), and serotonin type-3 receptors (2, 3). Individual Cys-loop receptor subunits consist of a large ligand-binding domain (LBD) and a transmembrane domain comprising four α-helices (TM1–TM4). LBDs themselves consist primarily of a "sandwich" of inner and outer β-sheets. The ligand binding site is situated at the interface of adjacent subunits and is formed by binding domain loops A–C from one subunit and loops D–F from the neighboring subunit (4).

The activation mechanism of Cys-loop receptors is the subject of considerable interest as it is important for understanding how this receptor family functions under normal and pathological conditions. Unwin (5) and co-workers (6) originally proposed that an agonist binding to its site induces loop C in the outer β-sheet to clasp tightly around the agonist. This is accompanied by a rotation of the inner β-sheet (5, 7–9). Abundant structural and functional evidence indicates that these conformational changes are transmitted to the transmembrane domain via a differential movement of loops 2 and 7 (both part of the inner β-sheet) and the pre-TM1 domain (which connects to the outer sheet) (3, 10–12). As loops 2 and 7 intercalate with the extracellular TM2-TM3 linker domain, agonist-induced movement of these loops alters the conformation of this linker, leading to channel gating.

Crystallography studies on acetylcholine-binding protein have shown that loop F of the outer sheet also moves upon ligand binding (13–15). However, there is as yet no consensus as to whether conformational changes in this loop represent local conformational changes to lock the ligand onto the binding site, simple distensions of the site to accommodate the ligand, or global conformational changes that are transmitted to the channel gate (16–19). Similarly, although agonists invariably induce loop C closure (5, 13–15), a direct link between loop C movement and channel opening has proved difficult to establish. Indeed, a recent study on the homomeric $\alpha1$ GlyR demonstrated that loop C conformational changes occur at high agonist concentrations only, raising the question of whether loop C closure is essential for receptor activation (18).

* This work was supported in part by the Australian Research Council and the National Health and Medical Research Council of Australia (NHMRC).
[1] Supported by a University of Queensland confirmation scholarship.
[2] Supported by an international postgraduate research scholarship from the University of Queensland. Present address: Dept. of Anesthesiology, Pharmacology and Therapeutics, University of British Columbia, Vancouver, British Columbia V6T 1Z3, Canada.
[3] Supported by an NHMRC research fellowship. To whom correspondence should be addressed. Tel.: 617-3346-6375; Fax: 617-3346-6301; E-mail: j.lynch@uq.edu.au.
[4] The abbreviations used are: $GABA_AR$, $GABA_A$ receptor; ΔF, change in fluorescence; ΔI, change in current; AF546, Alexa Fluor 546-C_5-maleimide; DMCM, methyl-6,7-dimethoxy-4-ethyl-β-carboline-3-carboxylate; GlyR, glycine receptor; LBD, ligand-binding domain; MTS-R, sulforhodamine methanethiosulfonate; MTS-TAMRA, 2-((5(6)-tetramethylrhodamine)carboxylamino)ethyl methanethiosulfonate; nAChR, nicotinic acetylcholine receptor; pre-M1, the domain preceding the first transmembrane segment; TMRM, tetramethylrhodamine-6-maleimide; VCF, voltage clamp fluorometry; Bis-Tris, 2-[bis(2-hydroxyethyl)amino]-2-(hydroxymethyl)-propane-1,3-diol.

The aim of the present study was to clarify the roles of loops C and F in channel activation using voltage clamp fluorometry (VCF). This technique correlates conformational changes occurring at the gate with those occurring in some other protein domain of interest in real time (20, 21). It takes advantage of the fact that rhodamine fluorescence exhibits an increase in quantum efficiency as the hydrophobicity of its environment is increased. Thus, rhodamine fluorescence intensity reports receptor conformational changes that alter its immediate chemical microenvironment. The unique advantages of VCF are that it can resolve movements in domains that are distant from the gate and detect conformational changes that are electrophysiologically silent. Indeed, VCF has provided valuable insights into the conformational rearrangements of various Cys-loop receptors (16–19, 22–29).

Attempts to date to define the roles of loops C and F using VCF have focused on homomeric ρ1 GABA$_A$Rs (16, 19, 30) and homomeric α1 GlyRs (18, 29). However, with homomeric receptors, it is not possible to discern whether or not fluorescence changes of fluorophores attached to loop C or F residues are restricted to those sites that contain bound ligands. In the present study, we used α1 β2 and α1 β2 γ2 GABA$_A$Rs in an attempt to compare conformational changes in loops C and F of each subunit that are induced by the agonists GABA and β-alanine, the antagonist gabazine (SR-95531), and the allosteric modulators diazepam and methyl-6,7-dimethoxy-4-ethyl-β-carboline-3-carboxylate (DMCM). The crucial advantage of GABA$_A$Rs over homomeric Cys-loop receptors is that GABA, β-alanine, and gabazine bind at LBD β-α interfaces only, whereas diazepam and DMCM bind with high affinity at LBD α-γ interfaces (31) and possibly to LBD α-β interfaces (see "Discussion"). In addition, a low affinity benzodiazepine site is also present in the transmembrane domain region of GABA$_A$Rs. Thus, by attaching fluorescent labels to loop C or F residues in one subunit only, we can discriminate between those conformational changes imposed by the immediate proximity of the ligand and those that are propagated to adjacent subunits and binding sites. We also investigated conformational changes in TM2-TM3 domain of each subunit to correlate conformational changes in loops C and F with those occurring at a more distant site along the gating pathway.

EXPERIMENTAL PROCEDURES

Reagents Used in VCF Experiments—Sulforhodamine methanethiosulfonate (MTS-R) and 2-((5(6)-tetramethylrhodamine)carboxylamino)ethyl methanethiosulfonate (MTS-TAMRA) were purchased from Toronto Research Chemicals (North York, Ontario, Canada). Alexa Fluor 546-C$_5$-maleimide (AF546) and tetramethylrhodamine-6-maleimide (TMRM) were purchased from Invitrogen. MTS-R, MTS-TAMRA, and TMRM were dissolved in dimethyl sulfoxide (DMSO) and stored at −20 °C. AF546 was dissolved directly into ND96 solution (96 mM NaCl, 2 mM KCl, 1 mM $MgCl_2$, 1.8 mM $CaCl_2$, 5 mM HEPES) on the day of the experiment and stored on ice for up to 6 h. GABA, β-alanine, and gabazine (Sigma-Aldrich) were dissolved in ND96 and stored at −20 °C. Diazepam and DMCM (both Sigma-Aldrich) were dissolved as 10 mM stocks in DMSO and stored at −20 °C. The 100:400 μM copper phenanthroline solution, which was used as an oxidizing agent, was generated by mixing copper sulfate and 1,10-phenanthroline in ND96 to final concentrations of 100 and 400 μM, respectively.

Molecular Biology—Rat α1, β2, and γ2 GABA$_A$R subunit cDNAs were subcloned into the pGEMHE plasmid vector. To eliminate uncross-linked extracellular cysteines, subunits incorporated the following background mutations: α1 subunit, C233S and C292S; β2 subunit, C287S; and γ2 subunit, C244S and C303A. QuikChange (Stratagene, La Jolla, CA) was used to generate all cysteine mutants used in this study. The successful incorporation of the mutations was confirmed by the automated sequencing of the entire coding sequence. Capped mRNA for oocyte injection was generated using mMessage mMachine (Ambion, Austin, TX).

Oocyte Preparation, Injection, and Labeling—Oocytes from female *Xenopus laevis* (*Xenopus* Express) were prepared as described previously (26) and injected with 10 ng of mRNA. The oocytes were then incubated at 18 °C for 3–7 days in an incubation solution containing 96 mM NaCl, 2 mM KCl, 1 mM $MgCl_2$, 1.8 mM $CaCl_2$, 5 mM HEPES, 0.6 mM theophylline, 2.5 mM pyruvic acid, and 50 μg/ml gentamycin (Cambrex Corp., East Rutherford, NJ), pH 7.4. On the day of recording, oocytes were transferred into ND96 containing 10–20 μM dye. Typical labeling times were 30 s for MTS-R and MTS-TAMRA (on ice), 30 min for TMRM (on ice), and 45 min for AF546 (at room temperature). Oocytes were washed thoroughly after labeling and stored in ND96 on ice for up to 6 h before recording. All four sulfhydryl-reactive fluorophores used in this study respond with an increase in quantum efficiency as the hydrophobicity of their environment is increased (22, 24, 30). Each cysteine mutant was incubated with all four fluorophores in turn, and the one yielding the largest change in fluorescence (ΔF) upon agonist application was analyzed. As unmutated α1 β2 dimeric or α1 β2 γ2 trimeric GABA$_A$Rs never exhibited a ΔF or a change in electrophysiological properties following fluorophore incubation, we can rule out nonspecific effects of the labels.

VCF and Data Analysis—The experimental setup comprised an inverted fluorescence microscope (IX51, Olympus, Tokyo, Japan) equipped with a high-Q tetramethylrhodamine isothiocyanate filter set (Chroma Technology, Rockingham, VT), a LUCPlanFLN 40×/numerical aperture 0.6 objective (Olympus), and a PhotoMax 200 photodiode (Dagan Corp., Minneapolis, MN) with a 12-V/100-watt halogen lamp (Olympus) as light source. The recording chamber is similar to those described previously (22, 30). Cells were voltage-clamped at −40 mV, and currents were recorded with an OC-725C oocyte amplifier (Warner, Hamden, CT). Current and fluorescence traces were acquired at 200 Hz via a Digidata 1322A interface using pClamp 9.2 software (Axon Instruments, Union City, CA). Fluorescence signals were digitally filtered at 1–2 Hz with an eight-pole Bessel filter for analysis and display. Half-maximal concentrations (EC_{50}) and Hill coefficient (n_H) values for ligand-induced activation of current and fluorescence were obtained using the Hill equation fitted with a non-linear least square algorithm (SigmaPlot 9.0, Systat Software, Point Richmond, CA). All results are ex-

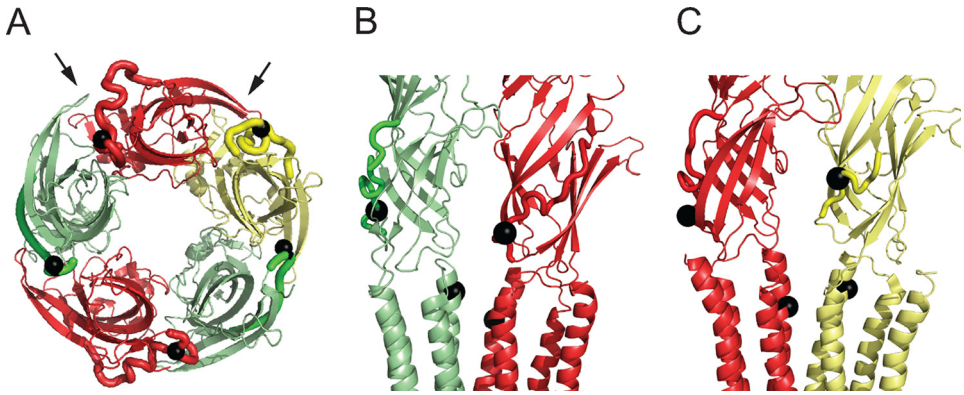

FIGURE 1. **Structural model of α1 β2 γ2 GABA$_A$R showing location of labeled sites investigated in this study.** The α1, β2, and γ2 subunits are colored *red*, *green*, and *yellow*, respectively. The loop F domains are shown as *thick lines*, and the positions of labeled residues in loop F and TM2-TM3 domain investigated in this study are depicted by the *black spheres*. *A*, view of the LBD looking axially outward from the membrane. The transmembrane domains have been removed for clarity. *Left* and *right arrows* show the direction of the view in *B* and *C*, respectively. *B*, interface between β2 and α1 subunits viewed from the direction shown in *A*. *C*, interface between α1 and γ2 subunits viewed from the direction shown in *A*.

pressed as mean ± S.E. of three or more independent experiments. Unless otherwise indicated, statistical analysis was performed using unpaired Student's *t* test with $p < 0.05$ representing significance.

Western Blotting—Oocytes were injected with 1 μg total of α1 and β2-K24′C subunit RNA in a 1:3 ratio. After 3 days of incubation, oocytes were washed once with ND96, and then some oocytes were treated with ND96 containing a 10 mM concentration of the reducing agent dithiothreitol (DTT). After 30 min of incubation with gentle shaking at 18 °C, DTT-treated oocytes were rinsed twice with ND96. After washing, DTT-treated and control oocytes were biotinylated in ND96 solution containing 1.22 mg/ml EZ-Link NHS-SS-biotin (succinimidyl 2-(biotinamido)-ethyl-1,3′-dithiopropionate; Pierce) for 60 min on ice accompanied by slow shaking. Oocytes were then washed twice with ND96 and gently pipetted at 4 °C in 20 μl of oocyte lysis buffer (comprising 0.1 M Tris-HCl pH 7.4 buffer, 1% Nonidet P-40, 0.3 M NaCl, 15 mM EDTA, 1 mM phenylmethanesulfonyl fluoride, and Complete Mini protease inhibitors, EDTA-free (Roche Diagnostics)) followed by several passages through a hypodermic syringe fitted with a 30-gauge needle. The resultant lysis mixture was sonicated three times for 20 s each on ice. To solubilize proteins from the membrane, Triton X (Sigma-Aldrich) was added to a final concentration of 1% to the sonicated cell mixture. The mixture was solubilized by rotating for 1 h at 4 °C. The lysate was then centrifuged at 50,000 × *g* for 30 min at 4 °C to remove debris and yolk. The resultant supernatant containing biotinylated proteins was transferred to streptavidin beads (Pierce) and rotated for 12–16 h at 4 °C. Beads were then washed with lysis buffer, and protein was eluted with 2× SDS loading buffer (no bromphenol blue/no DTT) plus 10 M urea. After concentration analysis using BCA Protein Assay kit (Pierce), bromphenol blue was added to both the control and DTT-treated samples, and 10 mM DTT was re-added to the DTT-treated sample. A total of 100 μg of protein from each sample was heated at 65 °C for 15 min before loading on a NuPAGE 4–12% Bis-Tris gel (Invitrogen) to separate. Protein bands were subsequently transferred to PVDF membrane by electrotransfer for 1 h using a Bio-Rad Mini Trans-Blot Electrophoretic Transfer Cell. PVDF membranes were blocked for 1 h with 3.5% skimmed milk in Tris-buffered saline containing 0.05% Tween 20 (Sigma-Aldrich) and processed with a primary rabbit anti-GABA$_A$R β2 polyclonal antibody (Millipore Bioscience Research Reagents) and subsequently with goat anti-rabbit HRP-conjugated secondary antibody (Santa Cruz Biotechnology, Santa Cruz, CA). PVDF membranes were developed using Super Signal West Pico (Pierce).

RESULTS

α1 Subunit Loop F—The GABA binding site lies at the interface of β2 and α1 subunits. Loop F of the α1 subunit is an unstructured domain that lines the base of the ligand binding pocket. In an attempt to clarify the role of this domain, we compared the conformational changes induced by agonists, antagonists, and a positive allosteric modulator in the loop F domains of α1, β2, and γ2 subunits. None of the drugs tested in this study produced a detectable ΔF response at unmutated α1 β2 or α1 β2 γ2 GABA$_A$Rs following incubation with any of the four fluorophores used in this study. We focused our investigation on the following cysteine-substituted residues: α1-R186C, β2-I180C, and γ2-S195C. Although the precise alignment between subunits in the loop F region is uncertain, any plausible alignment reveals that these three residues correspond closely. The locations of these residues on a GABA$_A$R structural model are shown in Fig. 1. Although we also attempted to investigate a range of other labeled sites in loop F, including A181C, E182C, D183C, G184C, and S185C in the α1 subunit and T175C, G176C, V177C, T178C, and K179C in the β2 subunit, mutant receptors incorporating these mutations did not produce significant ligand-induced ΔF responses following labeling with MTS-R, MTS-TAMRA, TMRM, or AF546.

The mean EC$_{50}$ of the GABA-activated change in current (ΔI) in α1-R186C β2 receptors was significantly higher ($p < 0.01$, unpaired *t* test) than that of unmutated α1 β2 GABA$_A$Rs (Table 1). Labeling with MTS-R resulted in a further rightward shift in the mean GABA ΔI EC$_{50}$ value and a significant ($p < 0.001$) reduction in peak current (ΔI_{max}), although the

TABLE 1

Summary of results obtained using GABA as agonist

Electrophysiological data are shown in regular type, and fluorescence data are shown in bold. —, not quantitated.

Construct	EC_{50}	n_H	I_{max} or ΔF_{max}	n
	μM			
α1 β2 unlabeled	0.8 ± 0.1	1.5 ± 0.1	9.5 ± 0.7 μA	5
α1 β2 MTS-R	0.7 ± 0.1	1.4 ± 0.1	8.9 ± 0.5 μA	5
α1 β2 γ2 unlabeled	3.2 ± 0.2	1.6 ± 0.1	9.6 ± 0.7 μA	4
α1 β2 γ2 MTS-R	3.5 ± 0.4	1.8 ± 0.1	10.3 ± 1.3 μA	4
α1-R186C β2 unlabeled	3.3 ± 0.2[a]	1.2 ± 0.1	7.4 ± 0.2 μA	3
α1-R186C β2 MTS-R	9.2 ± 1.1[b]	1.1 ± 0.1	2.6 ± 0.3 μA[b]	4
α1-R186C β2 MTS-R	**8.0 ± 0.7**	**0.8 ± 0.1**	**4.9 ± 0.4%**	**4**
α1 β2-I180C unlabeled	1.0 ± 0.1	1.3 ± 0.1	6.9 ± 1.2 μA	3
α1 β2-I180C MTS-TAMRA	1.1 ± 0.2	1.5 ± 0.1	7.5 ± 1.8 μA	4
α1 β2-I180C MTS-TAMRA	**1.0 ± 0.1**	**0.8 ± 0.1**	**1.5 ± 0.1%**	**4**
α1 β2 γ2-S195C unlabeled	2.9 ± 0.1	1.7 ± 0.03	10.1 ± 1.1 μA	4
α1 β2 γ2-S195C TMRM	6.1 ± 0.6[a]	1.6 ± 0.1	13.4 ± 1.7 μA	3
α1 β2 γ2-S195C TMRM	**3.8 ± 0.2**	**1.8 ± 0.4**	**1.7 ± 0.1%**	**3**
α1-N20′C β2 unlabeled	1.5 ± 0.2[c]	1.1 ± 0.1	8.1 ± 1.1 μA	3
α1-N20′C β2 TMRM	0.40 ± 0.03[a]	1.2 ± 0.2	6.1 ± 0.9 μA[c]	4
α1-N20′C β2 TMRM	—	—	**2.2 ± 0.4%**	**4**
α1-N20′C β2 γ2 unlabeled	14.2 ± 1.6[b]	1.1 ± 0.1	6.2 ± 1.0 μA[c]	3
α1-N20′C β2 γ2 TMRM	13.5 ± 0.5[b]	1.1 ± 0.1	8.3 ± 0.7 μA	4
α1-N20′C β2 γ2 TMRM	—	—	**0.8 ± 0.1%**	**4**
α1 β2-K24′C unlabeled	25.6 ± 4.2[b]	1.1 ± 0.1	1.6 ± 0.2 μA[b]	4
α1 β2-K24′C MTS-R	30.3 ± 3.8[b]	0.7 ± 0.1[b]	0.7 ± 0.1 μA[b]	4
α1 β2-K24′C MTS-R	**38.4 ± 3.8**	**0.90 ± 0.1**	**1.1 ± 0.1%**	**4**
α1 β2-K24′C γ2 unlabeled	91 ± 9[b]	1.1 ± 0.1	7.8 ± 1.4 μA	3
α1 β2-K24′C γ2 MTS-R	31.0 ± 2.3[b]	0.8 ± 0.1[b]	5.4 ± 1.2 μA[c]	4
α1 β2-K24′C γ2 MTS-R	**67 ± 1**	**0.8 ± 0.1**	**0.74 ± 0.02%**	**4**
α1 β2 γ2-P23′C unlabeled	2.7 ± 0.1	1.8 ± 0.1	9.2 ± 0.8 μA	5
α1 β2 γ2-P23′C TMRM	4.3 ± 0.7	1.7 ± 0.3	9.3 ± 0.3 μA	5
α1 β2 γ2-P23′C TMRM	—	—	**0.9 ± 0.1%**	**5**

[a] $p < 0.01$ relative to corresponding value at unlabeled α1 β2 $GABA_A$R using unpaired t test.
[b] $p < 0.001$ relative to corresponding value at unlabeled α1 β2 $GABA_A$R using unpaired t test.
[c] $p < 0.05$ relative to corresponding value at unlabeled α1 β2 $GABA_A$R using unpaired t test.

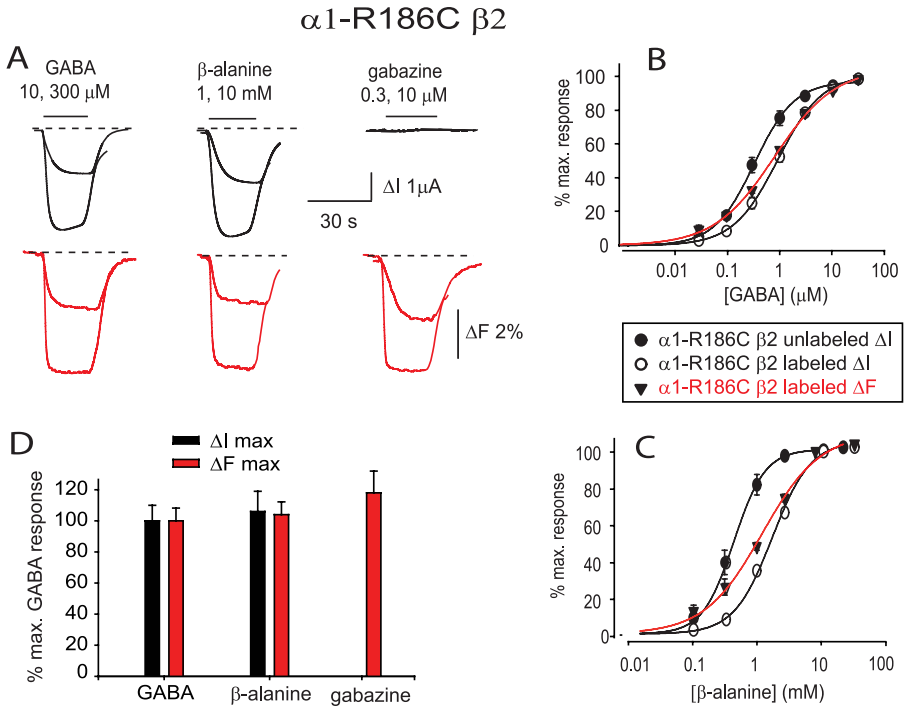

FIGURE 2. **Current and fluorescence responses recorded from unlabeled and MTS-R-labeled α1-R186C β2 $GABA_A$Rs.** *A*, current and fluorescence traces recorded from labeled α1-R186C β2 $GABA_A$Rs in response to the indicated concentrations of GABA, β-alanine, and gabazine. In this and subsequent figures, *black* traces denote current recordings, *red* traces denote fluorescence recordings, *horizontal bars* denote the duration of application of the indicated ligands, and *dashed lines* indicate the steady-state current or fluorescence levels observed in the absence of ligand. *B* and *C*, averaged GABA (*B*) and β-alanine (*C*) Δ*I* and Δ*F* concentration-response relationships at unlabeled and labeled α1-R186C β2 $GABA_A$Rs. *D*, comparison of ΔI_{max} (*black*) and ΔF_{max} (*red*) responses for GABA, β-alanine, and gabazine at the α1-R186C β2 $GABA_A$R. Data are normalized to the respective mean GABA values. *Error bars*, ± S.E.

n_H did not change (Table 1). A saturating (30 μM) GABA concentration produced a peak Δ*F* (ΔF_{max}) of 4.9% in α1-R186C β2 $GABA_A$Rs (Fig. 2*A* and Table 1). As MTS-R labeling of unmutated α1 β2 $GABA_A$Rs had no effect on the GABA Δ*I* EC_{50} or ΔI_{max} values (Table 1) and resulted in no detectable GABA-mediated Δ*F*, we conclude that R186C was specifically

TABLE 2

Summary of results obtained using β-alanine as agonist

Electrophysiological data are shown in regular type, and fluorescence data are shown in bold. —, not quantitated.

Construct	EC_{50}	n_H	I_{max} or ΔF_{max}	n
	mM			
α1 β2 unlabeled	0.05 ± 0.01	1.3 ± 0.1	7.2 ± 0.6 μA	5
α1 β2 γ2 unlabeled	0.97 ± 0.01	1.5 ± 0.1	12.5 ± 1.3 μA	4
α1-R186C β2 unlabeled	0.4 ± 0.1[a]	1.6 ± 0.4	6.5 ± 0.3 μA	3
α1-R186C β2 MTS-R	1.8 ± 0.1[b]	1.3 ± 0.1	3.2 ± 0.4 μA[b]	4
α1-R186C β2 MTS-R	**1.2 ± 0.1**	**0.9 ± 0.1**	**5.1 ± 0.4%**	**4**
α1 β2-I180C unlabeled	0.13 ± 0.02[a]	1.7 ± 0.2	7.2 ± 0.8 μA	3
α1 β2-I180C MTS-TAMRA	0.10 ± 0.01[b]	1.8 ± 0.1	7.8 ± 1.1 μA	3
α1 β2-I180C MTS-TAMRA	**0.10 ± 0.01**	**0.9 ± 0.1**	**1.3 ± 0.1%**	**3**
α1 β2 γ2-S195C unlabeled	1.23 ± 0.10[c]	1.8 ± 0.2	15.7 ± 0.5 μA	3
α1 β2 γ2-S195C TMRM	0.96 ± 0.05	2.2 ± 0.2[c]	15.1 ± 0.6 μA	3
α1 β2 γ2-S195C TMRM	—	—	**1.0 ± 0.1%**	**3**
α1-N20′C β2 unlabeled	0.14 ± 0.01[b]	1.2 ± 0.1	8.3 ± 1.2 μA	3
α1-N20′C β2 TMRM	0.07 ± 0.01	1.1 ± 0.1	7.8 ± 1.3 μA	3
α1-N20′C β2 TMRM	—	—	**1.7 ± 0.2%**	**3**
α1-N20′C β2 γ2 unlabeled	2.27 ± 0.10[b]	1.3 ± 0.1	8.6 ± 1.0 μA	3
α1-N20′C β2 γ2 TMRM	0.86 ± 0.10	1.1 ± 0.1	7.5 ± 0.2 μA[a]	4
α1-N20′C β2 γ2 TMRM	—	—	**0.5 ± 0.1%**	**4**
α1 β2-K24′C unlabeled	3.1 ± 0.1[b]	1.3 ± 0.1	2.6 ± 0.5 μA[b]	4
α1 β2-K24′C MTS-R	5.4 ± 1.0[b]	0.8 ± 0.1[a]	1.2 ± 0.1 μA[b]	4
α1 β2-K24′C MTS-R	**3.6 ± 0.2**	**0.90 ± 0.1**	**0.9 ± 0.1%**	**4**
α1 β2-K24′C γ2 unlabeled	9.8 ± 0.9[b]	1.2 ± 0.1	5.6 ± 1.1 μA[a]	4
α1 β2-K24′C γ2 MTS-R	4.9 ± 0.5[b]	0.9 ± 0.03[a]	6.1 ± 1.2 μA[c]	4
α1 β2-K24′C γ2 MTS-R	**10.0 ± 1.6**	**0.7 ± 0.1**	**0.6 ± 0.1%**	**4**
α1 β2 γ2-P23′C unlabeled	1.14 ± 0.04	1.6 ± 0.1	10.7 ± 0.7 μA	3
α1 β2 γ2-P23′C TMRM	1.38 ± 0.04	2.0 ± 0.2[c]	9.5 ± 0.5 μA	5
α1 β2 γ2-P23′C TMRM	—	—	**1.0 ± 0.1%**	**5**

[a] $p < 0.01$ relative to corresponding value at unlabeled α1 β2 GABA$_A$R using unpaired *t* test.
[b] $p < 0.001$ relative to corresponding value at unlabeled α1 β2 GABA$_A$R using unpaired *t* test.
[c] $p < 0.05$ relative to corresponding value at unlabeled α1 β2 GABA$_A$R using unpaired *t* test.

covalently labeled by rhodamine. We were unable to detect a significant Δ*F* following labeling of α1-R186C β2 receptors with AF546 or TMRM, although a small GABA-evoked Δ*F* was observed following labeling with MTS-TAMRA. The on and off time courses of Δ*F* responses generally correlated well with agonist application and removal (Fig. 2*A*). However, because currents are recorded from the entire oocyte and fluorescence is recorded only from a small surface area, slight discrepancies between current and fluorescence on and off rates are expected. After normalization, the Δ*I* and Δ*F* concentration-response relationships of MTS-R-labeled α1-R186C β2 GABA$_A$Rs were almost superimposed (Fig. 2*B*) with the averaged Δ*I* and Δ*F* EC_{50} values showing no significant difference ($p > 0.05$; Table 1).

β-Alanine is a low affinity full agonist of the GABA$_A$R (32). As with GABA-mediated responses, MTS-R labeling of the α1-R186C β2 GABA$_A$R resulted in a rightward shift in the mean β-alanine Δ*I* EC_{50} value (Fig. 2*C*) that was also accompanied by a significant reduction in ΔI_{max} ($p < 0.001$; Table 1). Saturating (10 mM) β-alanine concentrations produced ΔF_{max} values comparable in magnitude with those produced by GABA (Fig. 2*A* and Table 1). As with GABA-mediated responses, the averaged β-alanine Δ*I* and Δ*F* dose-response relationships were largely overlapping in these receptors (Fig. 2*C* and Table 2).

Gabazine is a high affinity competitive antagonist of GABA$_A$Rs (33). One previous VCF study showed that gabazine and GABA elicited different conformation changes in the GABA$_A$R α1 subunit loop E domain (24), although the F loop has yet to be investigated. Another showed that agonists and competitive antagonists evoked distinct ΔF_{max} responses at several labeled loop F residues in homomeric ρ1 GABA$_A$Rs (16). Our own VCF study on homomeric α1 GlyRs showed that the agonist glycine and the competitive antagonist strychnine elicited distinct ΔF_{max} responses in loops C, D, and E but identical ΔF_{max} responses at two labeled loop F sites (18). Consistent with our previous GlyR results, in the present study, we found that gabazine produced a ΔF_{max} that was similar in magnitude and direction to that elicited by the agonists (Fig. 2*A*). The mean gabazine Δ*F* EC_{50} was 0.4 ± 0.02 μM, the n_H was 1.1 ± 0.1, and ΔF_{max} was 5.8 ± 0.7% (all averaged from $n = 4$ oocytes). A comparison of mean ΔF_{max} and ΔI_{max} values for GABA, β-alanine, and gabazine at the α1-R186C β2 GABA$_A$Rs reveals no significant difference in their ΔF_{max} responses (Fig. 2*D*). This result provides no evidence for GABA, β-alanine, and gabazine inducing different conformational changes in this domain. Although α1 β2 GABA$_A$Rs contain a low affinity benzodiazepine binding site (34), we found that concentrations of diazepam up to 100 μM, applied in the presence of 3 μM (EC_{20}) GABA, elicited no detectable Δ*F* response in the MTS-R-labeled α1-R186C β2 GABA$_A$R.

β2 Subunit Loop F—The β2-I180C mutation had no significant effect on GABA sensitivity of α1 β2 GABA$_A$Rs (Table 1). Although incubation with MTS-R did not result in a detectable GABA-mediated Δ*F*, MTS-TAMRA-labeled α1 β2-I180C GABA$_A$Rs elicited a GABA-mediated ΔF_{max} of about 1.5% (Fig. 3*A*). MTS-TAMRA labeling had no significant effect on the GABA Δ*I* EC_{50}, n_H, or ΔI_{max} values (Fig. 3*B* and Table 1). The GABA Δ*I* and Δ*F* concentration-response relationships were largely overlapping with no significant difference in their respective EC_{50} values ($p > 0.05$; Fig. 3*B* and Table 1). There was, however, a dramatic reduction in the mean n_H of the Δ*F* relative to the Δ*I* and concentration-response relationship ($p < 0.01$; Table 1).

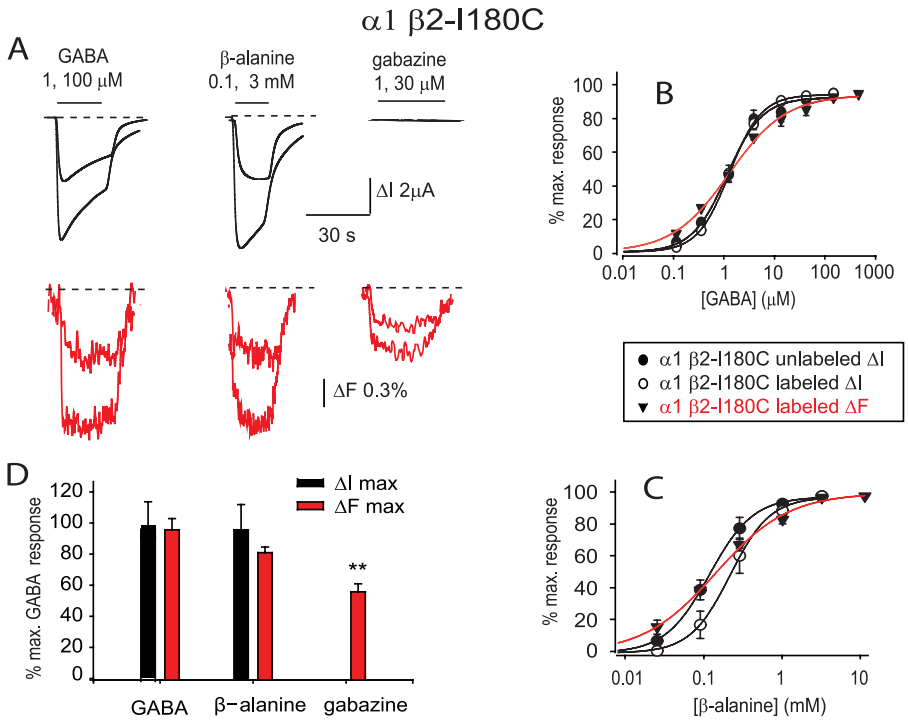

FIGURE 3. **Current and fluorescence responses recorded from unlabeled and MTS-TAMRA-labeled α1 β2-I180C GABA$_A$Rs.** *A*, current and fluorescence traces recorded from labeled α1 β2-I180C GABA$_A$Rs in response to the indicated concentrations of GABA, β-alanine, and gabazine. *B* and *C*, averaged GABA (*B*) and β-alanine (*C*) Δ*I* and Δ*F* concentration-response relationships at unlabeled and labeled α1 β2-I180C GABA$_A$Rs. *D*, comparison of ΔI_{max} (*black*) and ΔF_{max} (*red*) responses for GABA, β-alanine, and gabazine at the α1 β2-I180C GABA$_A$R. Data are normalized to mean GABA values. **, $p < 0.01$ relative to corresponding GABA value by unpaired *t* test. *Error bars*, ± S.E.

Receptor sensitivity to β-alanine was significantly ($p < 0.01$) decreased in the α1 β2-I180C mutant relative to the unmutated GABA$_A$R (Table 2), but there was no β-alanine ΔI or Δ*F* EC_{50} difference between unlabeled and MTS-TAMRA-labeled mutant receptors (Fig. 3*C* and Table 2). The ΔF_{max} elicited by β-alanine reached 1.3%, which is comparable with the value induced by GABA (Fig. 3*A*). As with the GABA-mediated responses, the β-alanine-evoked Δ*I* and Δ*F* concentration-response relations were largely overlapping with no significant difference in their respective EC_{50} values ($p > 0.05$; Table 2). Notably, however, the β-alanine Δ*F* n_H value was dramatically reduced relative to that of Δ*I* ($p < 0.001$; Table 2). A Δ*F* signal was also observed following application of gabazine, although the ΔF_{max} was significantly smaller than that induced by GABA ($p < 0.01$; Fig. 3, *A* and *D*). The EC_{50} of the gabazine Δ*F* concentration-response curve was 0.67 ± 0.03 μM, n_H was 1.3 ± 0.1, and ΔF_{max} was 0.8 ± 0.1% (all n = 4 oocytes). As loop F of the β2 subunit does not contribute to the agonist binding site, the ligand-induced conformational rearrangements seen in this domain cannot be due to a direct ligand-fluorophore interaction. Thus, we conclude that all three ligands produce allosteric conformational changes to this domain with those of GABA and β-alanine being different from that of gabazine. Although α1 β2 GABA$_A$Rs contain a low affinity benzodiazepine binding site (34), we found that concentrations of diazepam up to 100 μM, applied in the presence of 0.3 μM (EC_{20}) GABA, elicited no detectable Δ*F* response in the MTS-TAMRA-labeled α1 β2-I180C GABA$_A$R.

γ2 Subunit Loop F—When co-expressed with α1 and β2 subunits, the γ2 subunit increased the Δ*I* EC_{50} values of GABA and β-alanine dramatically, providing strong evidence for the incorporation of these subunits into trimeric α1 β2 γ2 GABA$_A$Rs (Table 1). Arg-197 in loop F of the γ2 subunit is homologous with α1-Arg-186 and is thought to be important for diazepam binding (35).

Unfortunately, α1 β2 γ2 GABA$_A$Rs incorporating the mutation R194C, W196C, or R197C to the γ2 subunit showed no evidence for labeling by any of the four tested fluorophores. However, the α1 β2 γ2-S195C GABA$_A$R was productively labeled by TMRM. The mutation itself produced no significant change in the GABA or β-alanine Δ*I* EC_{50} values (Tables 1 and 2). Labeling with TMRM significantly increased the GABA Δ*I* EC_{50} value ($p < 0.01$; Table 1) and gave rise to a small (1.7%) GABA-induced ΔF_{max} (Fig. 4, *A* and *B*). The GABA Δ*F* EC_{50} value was slightly left-shifted relative to that of Δ*I* (Table 1). In contrast, TMRM labeling resulted in a modest decrease in the mean β-alanine Δ*I* EC_{50} value (Table 2). The β-alanine-mediated ΔF_{max} value was 1.0%, which was significantly smaller than that produced by GABA ($p < 0.01$; Table 2). The small size of this signal precluded quantitation of the full β-alanine Δ*F* concentration-response relationship. We did not detect a significant gabazine-induced Δ*F*. Taken together, several observations, including the non-overlapping GABA Δ*I* and Δ*F* concentration-response relationships and the differing effects of the γ2-S195C mutation on GABA and β-alanine Δ*I* EC_{50} values coupled with their significantly different ΔF_{max} values (Fig. 4*B*), suggest that GABA and β-alanine produced different conformational changes at this residue.

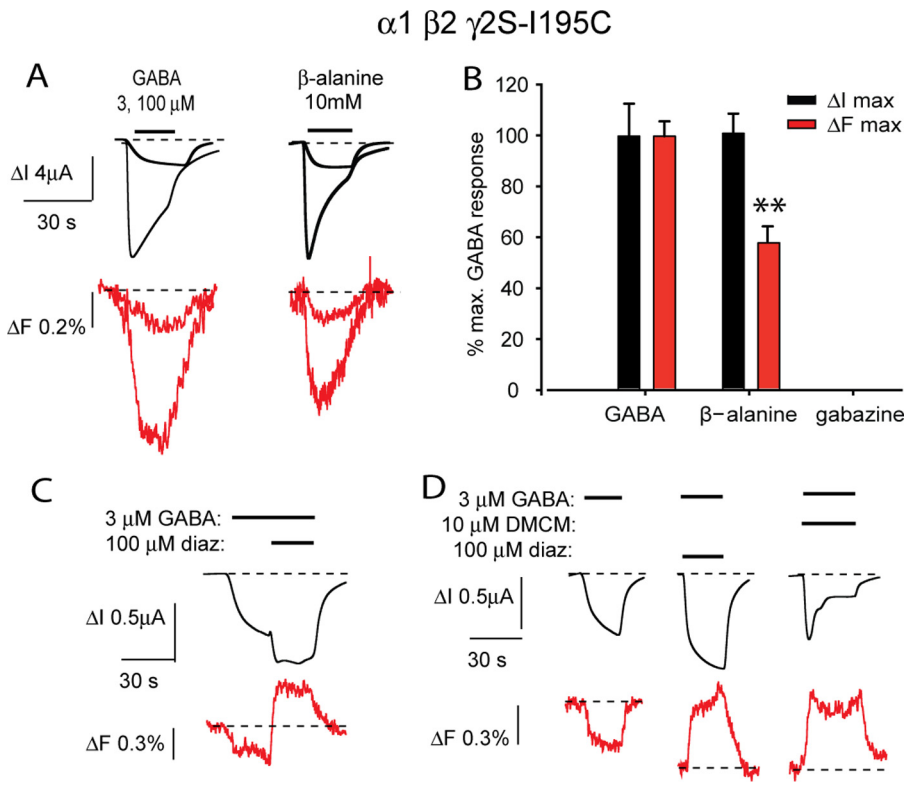

FIGURE 4. **Current and fluorescence responses recorded from TMRM-labeled α1 β2 γ2-I195C GABA$_A$Rs.** *A*, current and fluorescence traces recorded in response to the indicated concentrations of GABA and β-alanine. *B*, comparison of ΔI_{max} (*black*) and ΔF_{max} (*red*) responses for GABA, β-alanine, and gabazine. **, $p < 0.01$ relative to corresponding GABA value by unpaired *t* test. *C* and *D*, sample current and fluorescence traces recorded in response to the indicated concentrations of GABA, diazepam (*diaz*), and DMCM. *Error bars*, ± S.E.

As the γ2 subunit loop F contributes to the binding site for diazepam and DMCM (31), we investigated the actions of both compounds on the α1 β2 γ2-S195C GABA$_A$R. Because diazepam has both a high affinity site that requires the γ2 subunit and a low affinity site that does not (34), we applied 10 and 100 μM concentrations of diazepam both alone and together with 3 μM (EC_{30}) GABA in an attempt to distinguish between the effects of diazepam occupying the low and high affinity sites. Application of diazepam alone at either concentration produced no detectable Δ*I* or Δ*F*. However, when co-applied with GABA, both diazepam concentrations produced a small Δ*F* (0.33 ± 0.05%, $n = 5$ oocytes) that was opposite in sign to those produced by GABA and β-alanine at the same labeled site (Fig. 4, *C* and *D*). Control experiments confirmed that all Δ*F* signals reported in this study were not mediated by the DMSO used to dissolve the drugs (not shown). A 10 μM concentration of DMCM blocked 42 ± 3% ($n = 5$ oocytes) of the Δ*I* induced by 3 μM GABA (*e.g.* Fig. 4*D*), and the accompanying ΔF_{max} was of the same sign as that produced by diazepam but was slightly larger (0.50 ± 0.01%, $n = 5$ oocytes). These results suggest that GABA and β-alanine induce an allosteric conformational change in the γ2 subunit F loop region, whereas diazepam and DMCM elicit a distinct local conformational change. We also investigated the effects of 100 μM diazepam on MTS-R-labeled α1-R186C β2 γ2 and MTS-TAMRA-labeled α1 β2-I180C γ2 GABA$_A$Rs but observed no significant Δ*F* at either receptor ($n = 5$ oocytes for each experiment; not shown).

Loop C—As β2 and α1 loop C residues are directly involved in coordinating GABA and benzodiazepines, respectively (31), we introduced cysteine mutations one at a time only to those loop C residues that are not involved in ligand binding. The mutations we introduced were as follows: α1 subunit: Q203C, S204C, G207C*, and E208C; β2 subunit: S200C, T201C, G202C*, and S203C; and γ2 subunit: K214C, T216C, and G228C. Asterisks denote those mutations that prevented the expression of GABA-mediated currents. Mutated α1 subunits were expressed as dimers with unmutated β2 subunits or as trimers with unmutated β2 and unmutated γ2 subunits. Similarly, mutated β2 subunits were expressed with unmutated α1 subunits with or without unmutated γ2 subunits. Mutated γ2 subunits were expressed as trimers with unmutated α1 and β2 subunits. Oocytes injected with each of these subunit combinations were incubated with each of the four fluorophores in turn. Unfortunately, none of the incubated receptors responded with a detectable Δ*F* when challenged by saturating concentrations of GABA, β-alanine, gabazine, or diazepam.

α1 Subunit TM2-TM3 Domain—The TM2-TM3 linker is an extracellular domain that interacts closely with loops 2, 7, and 9 of the ligand-binding domain (3, 11). To allow for comparison of TM2 residues among different Cys-loop receptors, a residue numbering system is used that assigns 1′ to the innermost TM2 residue and 19′ to the residue at the external lipid-water interface that forms the start of the TM2-TM3 linker. As the TM2-TM3 domain lies distant from the ligand binding sites and forms a critical component of the channel

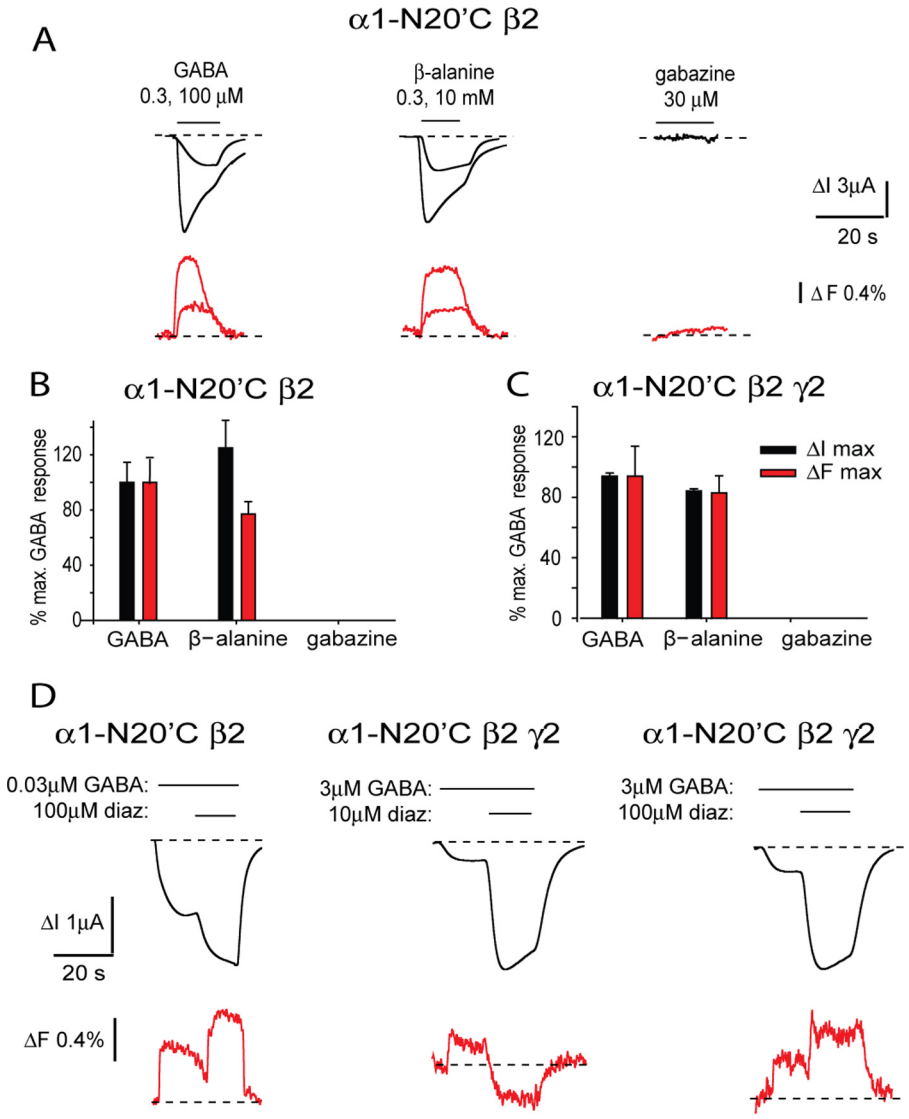

FIGURE 5. **Current and fluorescence responses recorded from GABA$_A$Rs incorporating TMRM-labeled α1-N20′C subunits.** *A*, current and fluorescence traces recorded from α1-N20′C β2 GABA$_A$Rs in response to the indicated concentrations of GABA, β-alanine, and gabazine. *B* and *C*, comparison of ΔI_{max} (*black*) and ΔF_{max} (*red*) responses for GABA, β-alanine, and gabazine at the α1-N20′C β2 (*B*) and α1-N20′C β2 γ2 (*C*) GABA$_A$Rs. Data are normalized to mean GABA values. Note the complete absence of gabazine responses in *B* and *C*. *D*, current and fluorescence traces recorded from α1-N20′C β2 GABA$_A$Rs and α1-N20′C β2 γ2 GABA$_A$Rs in response to the indicated concentrations of GABA and diazepam (*diaz*). GABA was applied at the EC_{10} concentration for each receptor. *Error bars*, ± S.E.

opening mechanism (36–38), we compared the actions of the agonists, allosteric modulators, and antagonists in inducing conformational changes in this region. Although we attempted to label all cysteine-substituted residues from 19′ to 27′ in the α1 subunit M2-M3 domain using each of the four dyes, robust ligand-mediated Δ*F* responses were observed only when N20′C (Fig. 1) was labeled with TMRM (Fig. 4*A*). The α1-N20′C β2 GABA$_A$R exhibited a small increase in the GABA and β-alanine Δ*I* EC_{50} values relative to the unmutated receptor, although for both agonists, this increase was reversed after labeling with TMRM (Tables 1 and 2). Oocytes expressing α1-N20′C β2 GABA$_A$Rs produced saturating GABA- and β-alanine-evoked ΔF_{max} of values near 2% (Fig. 5*A* and Tables 1 and 2). It was not possible to quantitate agonist Δ*F* concentration-response relationships as the Δ*F* signal appeared to run down dramatically after an initial agonist application. Possible explanations for this phenomenon are considered below. The β-alanine-induced ΔI_{max} and initial ΔF_{max} values were similar in magnitude to those elicited by GABA (Fig. 5, *A* and *B*). Application of saturating (30 μM) gabazine did not produce a detectable Δ*F* signal (Fig. 5, *A* and *B*). Thus, the conformational change reported by this Δ*F* signal is restricted to agonists, implying that this receptor region may be involved in gating.

TMRM labeling of trimeric α1-N20′C β2 γ2 GABA$_A$Rs significantly increased the agonist sensitivity to β-alanine ($p < 0.001$) but not to GABA ($p > 0.05$; Tables 1 and 2). The ΔF_{max} values induced by either GABA or β-alanine were significantly reduced in magnitude ($p = 0.01$ and $p < 0.001$, respectively) following γ2 subunit incorporation (Tables 1 and 2), whereas saturating gabazine still elicited no Δ*F* response (Fig. 5*C*). We next investigated whether diazepam alters the conformation of the α1 subunit TM2-TM3 domain. As shown in the example in Fig. 5*D*, the magnitude of the Δ*I* increase

produced by 100 μM diazepam in the presence of 3 μM (EC_{10}) GABA in the α1-N20′C β2 γ2 $GABA_AR$ was 1.8-fold larger (representative of $n = 4$ recordings) than that produced in the presence of an equivalent (EC_{10}) GABA concentration in the α1-N20′C β2 $GABA_AR$. As shown in the sample traces in Fig. 5*D*, in the α1-N20′C β2 $GABA_AR$ and α1-N20′C β2 γ2 $GABA_AR$, 100 μM diazepam produced a mean increase in ΔF of 0.66 ± 0.01 and 0.30 ± 0.01% (both $n = 4$ oocytes), respectively. However, in the α1-N20′C β2 γ2 $GABA_AR$, 10 μM diazepam produced a mean decrease in ΔF of 0.55 ± 0.13% ($n = 4$ oocytes). Application of either diazepam or DMSO alone did not produce a detectable ΔF signal. This result suggests that diazepam induces a different conformational change depending on whether it is binding to its high or low affinity sites.

β2 Subunit TM2-TM3 Domain—To investigate the role of the β2 subunit TM2-TM3 domain, we were able to successfully label K24′C with MTS-R (Fig. 1). Application of GABA or β-alanine to α1 β2-K24′C $GABA_ARs$ produced a robust increase in ΔF (Fig. 6*A*). Relative to the unmutated receptor, the α1 β2-K24′C mutant $GABA_AR$ exhibited a dramatic increase in GABA and β-alanine ΔI EC_{50} values and a dramatic decrease in their respective ΔI_{max} values ($p < 0.001$ for both; Tables 1 and 2). Labeling with MTS-R modestly increased the GABA ΔI EC_{50} value (Fig. 6*B*) but not the β-alanine ΔI EC_{50} value (Fig. 6*B*) and reduced the ΔI_{max} values even further by around 50% for both agonists ($p < 0.001$; Tables 1 and 2). MTS-R labeling also produced significant decreases in the n_H values for both agonists ($p < 0.001$; Tables 1 and 2) Saturating concentrations of GABA and β-alanine induced ΔF_{max} values of 1.1 and 0.9%, respectively (Tables 1 and 2). The concentration-response curves of GABA- and β-alanine-mediated ΔI and ΔF responses were almost overlapping (Fig. 6, *B* and *C*) with their respective ΔI and ΔF EC_{50} values showing no significant difference from each other ($p > 0.05$ for both GABA and β-alanine; Tables 1 and 2). After labeling, ΔI_{max} values induced by β-alanine were significantly larger than the current induced by saturating GABA ($p < 0.05$), but there was no significant difference in their respective ΔF_{max} values ($p > 0.05$; Tables 1 and 2). As suggested by the example in Fig. 6*A* and confirmed by the averaged results summarized in Fig. 6*D*, a 30 μM concentration of gabazine evoked a negative ΔF signal. Together, these results suggest that the labeled β2-K24′C residue reports a conformational change associated with channel opening and that gabazine produces an allosteric conformational change distinct from that induced by agonists.

When incorporated into the α1 β2-K24′C $GABA_AR$, the γ2 subunit produced the expected rightward shift in the GABA and β-alanine ΔI EC_{50} values that was accompanied by a dramatic increase in their respective ΔI_{max} values (Tables 1 and 2). Labeling with MTS-R induced modest increases in α1 β2-K24′C γ2 $GABA_AR$ sensitivity to GABA and β-alanine (Fig. 6, *E* and *F*), significant decreases in the n_H values for both agonists (Tables 1 and 2), and no change in their respective ΔI_{max} values ($p > 0.05$ for GABA and β-alanine; Tables 1 and 2). The ΔF_{max} responses activated by GABA and β-alanine were significantly smaller than those observed in the dimeric α1 β2-K24′C $GABA_AR$ ($p < 0.01$ for GABA and $p < 0.05$ for

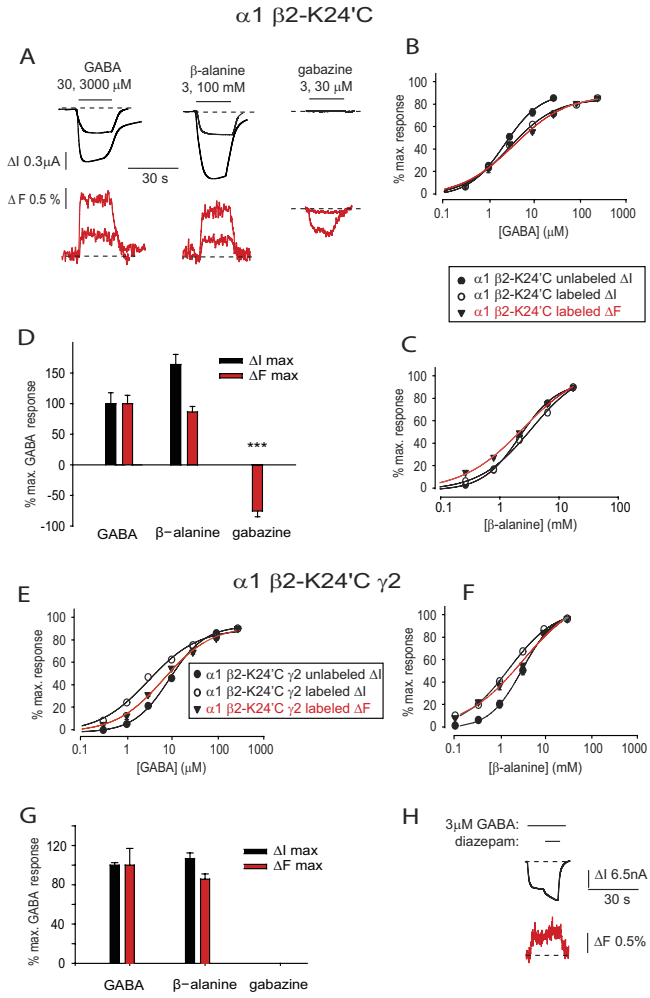

FIGURE 6. **Current and fluorescence responses recorded from $GABA_ARs$ incorporating MTS-R-labeled β2-K24′C subunits.** *A*, current and fluorescence traces recorded from α1 β2-K24′C $GABA_ARs$ in response to the indicated concentrations of GABA, β-alanine, and gabazine. *B* and *C*, averaged concentration-response relationships for GABA (*B*) and β-alanine (*C*) at the α1 β2-K24′C $GABA_AR$. *D*, comparison of ΔI_{max} (*black*) and ΔF_{max} (*red*) responses for GABA, β-alanine, and gabazine at the α1 β2-K24′C $GABA_AR$. Data are normalized to mean GABA values. ***, $p < 0.001$ by unpaired *t* test. *E* and *F*, averaged concentration-response relationships for GABA (*E*) and β-alanine (*F*) at the α1 β2-K24′C γ2 $GABA_AR$. *G*, comparison of ΔI_{max} (*black*) and ΔF_{max} (*red*) responses for GABA, β-alanine, and gabazine at the α1 β2-K24′C γ2 $GABA_AR$. Data are normalized to mean GABA values. Note the lack of response to gabazine. *H*, current and fluorescence traces recorded from α1 β2-K24′C γ2 $GABA_ARs$ in response to the indicated concentrations of GABA and diazepam. *Error bars*, ± S.E.

β-alanine; Tables 1 and 2), probably reflecting the reduced abundance of β2-K24′C subunits. As summarized in Fig. 6*G*, the ΔF_{max} responses of β-alanine and GABA were not significantly different from each other. Incorporation of γ2 subunits resulted in small but significant (*, $p < 0.05$) increases in GABA and β-alanine ΔF EC_{50} values relative to their corresponding ΔI EC_{50} values (Fig. 6, *E* and *F*, and Tables 1 and 2). Because of their small size, we were unable to analyze the ΔF signals induced by gabazine and diazepam in α1 β2-K24′C γ2 $GABA_ARs$ (*e.g.* Fig. 6*H*).

Because insertion of the γ2 subunit dramatically increased ΔI_{max} (*e.g.* Fig. 7*A*), we hypothesized that two adjacent β2-K24′C subunits might cross-link to form a disulfide bond that holds the channel closed. Disulfide cross-links between adja-

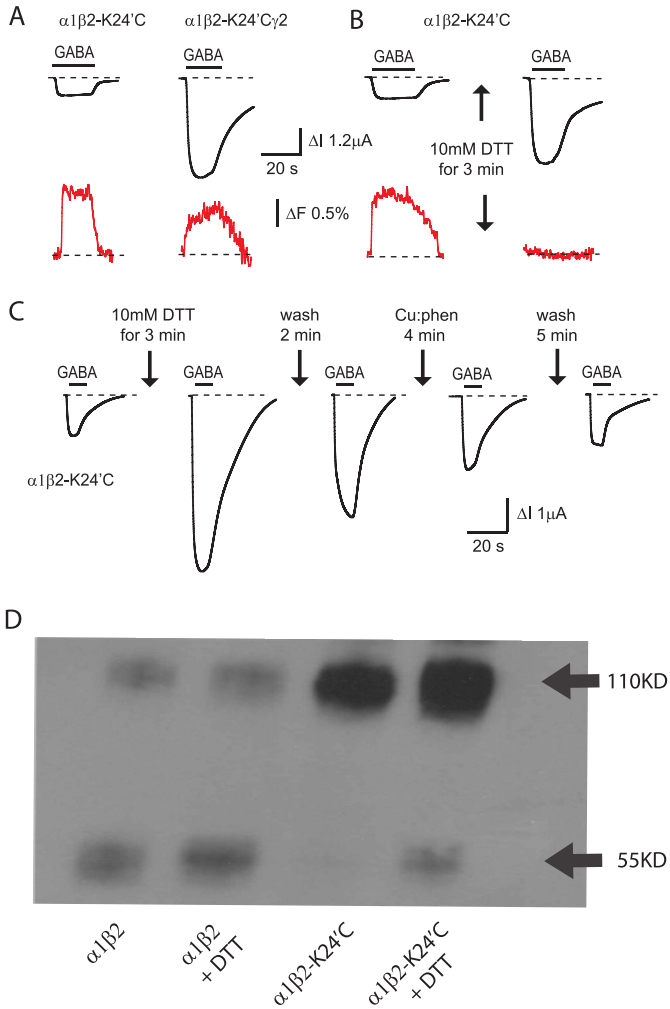

FIGURE 7. **Disulfide bond formation between adjacent β2-K24′C residues.** *A*, incorporation of a γ2 subunit, which precludes the formation of adjacent β2-K24′C subunits, dramatically increases the ΔI_{max} activated by saturating (100 μM) GABA while having little effect on ΔF_{max}. See text and Tables 1 and 2 for averaged ΔI_{max} and ΔF_{max} values. *B*, all traces were recorded from the same oocyte expressing α1 β2-K24′C GABA$_A$Rs. A 3-min application of 10 mM DTT dramatically increases saturating current magnitude. Note that the Δ*F* signal disappears presumably due to reduction of the disulfide bond linking rhodamine to K24′C. *C*, all traces were recorded from the same oocyte expressing α1 β2-K24′C GABA$_A$Rs. The DDT-mediated current increase reverses spontaneously, and this is enhanced by application of 100:400 μM copper phenanthroline (*Cu:phen*). *D*, Western blot of α1 β2 and α1 β2-K24′C GABA$_A$Rs with molecular masses as indicated. *Lanes 1* and *2* show that α1 β2 GABA$_A$Rs exist primarily as monomers with a small dimer population with the relative quantity of monomer increasing with DTT treatment. *Lanes 3* and *4* show that α1 β2-K24′C GABA$_A$Rs exist mainly as dimers with a weak monomer band that increased in intensity following DTT treatment. This result was representative of four independent experiments using different protein samples. In all four experiments, monomer labeling appeared much weaker than dimer labeling possibly due to reduced epitope exposure.

cent β2 subunits via cysteines introduced at the 6′ and 20′ positions have previously been shown to prevent GABA$_A$R activation (39–42). To test this hypothesis, we applied a 10 mM concentration of the reducing agent, DTT, for 3 min to MTS-R-labeled α1 β2-K24′C GABA$_A$Rs. As shown in Fig. 7*B*, a dramatic increase in GABA-activated current was observed (from 0.7 ± 0.1 to 6.5 ± 0.5 μA, $n = 4$ oocytes) that was accompanied by the complete loss of the Δ*F* signal. The loss in Δ*F* was most likely due to the DTT-mediated reduction of the disulfide bond attaching rhodamine to K24′C. The increased current was most likely due to the reduction of an inter-β subunit disulfide bond in a different population of receptors from those labeled by rhodamine. We tested this by applying 10 mM DTT for 3 min to unlabeled α1 β2-K24′C GABA$_A$Rs (Fig. 7*C*) whereupon the current activated by 100 μM GABA increased >10-fold (from 0.34 ± 0.02 to 4.4 ± 0.5 μA, $n = 4$ oocytes), which is significantly more than the increase observed in labeled receptors ($p < 0.05$). We interpret the enhanced current increase as being due to a smaller initial control current caused by the cross-linking of a larger proportion of receptors. Following DTT exposure, the current recovered slightly following a 2-min wash in control solution (Fig. 7*C*). However, application of 100:400 μM copper phenanthroline (an oxidizing agent) accelerated the current recovery (Fig. 7*C*). The opposing effects of oxidizing and reducing agents on current magnitude suggests that two adjacent β2-K24′C subunits form a disulfide bond in the closed state that holds the channel closed. As shown in Fig. 7*D*, Western blot analysis supports this conclusion. The unmutated α1 β2 GABA$_A$R exhibited a dominant monomer band (55 kDa) and a weaker dimer band (110 kDa) with the relative quantity of monomer increasing following DTT treatment (Fig. 7*D*). In contrast, the α1 β2-K24′C GABA$_A$R displayed a much more dominant dimer band and a weaker monomer band that also increased in intensity following DTT treatment (Fig. 7*D*). This Western blot result was replicated in four independent experiments. In all four experiments, monomer labeling appeared much weaker than dimer labeling possibly due to reduced epitope exposure. Together, these data provide strong evidence for the dimerization of adjacent β-K24′C subunits.

γ2 Subunit TM2-TM3 Domain—Cysteines introduced at 20′ and 24′ positions of the γ2 subunit produced no significant GABA- or diazepam-dependent Δ*F* responses, whereas P23′C was productively labeled with TMRM. Its location is shown in Fig. 1. Mutant α1 β2 γ2-P23′C receptors exhibited GABA and β-alanine Δ*I* EC_{50} and ΔI_{max} values that were indistinguishable from those of unmutated α1 β2 γ2 GABA$_A$Rs (Tables 1 and 2). Following incubation with TMRM for 30 min, the mean Δ*I* EC_{50} values for both GABA and β-alanine were slightly increased relative to those of unlabeled α1 β2 γ2-P23′C GABA$_A$Rs (Tables 1 and 2). The ΔF_{max} values induced by saturating GABA and β-alanine were both near 1% (Fig. 8*A* and Tables 1 and 2), but gabazine produced no detectable Δ*F* (Fig. 8*B*). As shown in Fig. 8*A*, 10 μM diazepam produced an increase in both Δ*I* and Δ*F* when co-applied with 3 μM (EC_{35}) GABA. In this experiment, GABA alone produced a mean Δ*I* of 2.4 ± 0.3 μA and a Δ*F* of 0.17 ± 0.01% (both $n = 4$), whereas diazepam co-application increased the Δ*I* to 3.0 ± 0.2 μA and the Δ*F* to 0.37 ± 0.01% in the same four oocytes. Using a paired *t* test, the increase in Δ*F* was statistically significant ($p < 0.05$), whereas the increase in Δ*I* was not ($p > 0.05$).

DISCUSSION

General Considerations for Data Interpretation—An agonist-induced Δ*F* implies that the microenvironment of an at-

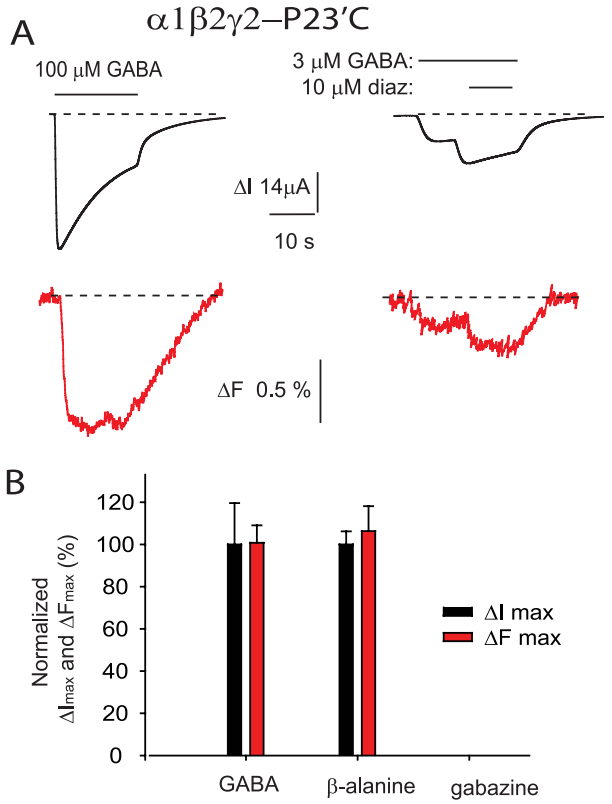

FIGURE 8. **Current and fluorescence responses recorded from TMRM labeled α1 β2 γ2-P23′C GABA$_A$Rs.** *A*, current and fluorescence traces recorded in response to the indicated concentrations of GABA and diazepam (*diaz*). *B*, comparison of ΔI_{max} (*black*) and ΔF_{max} (*red*) responses for GABA, β-alanine, and gabazine at the α1 β2 γ2-P23′C GABA$_A$R. Data are normalized to mean GABA values. Note the lack of responses to gabazine. *Error bars*, ± S.E.

tached fluorophore has been chemically altered as a result of agonist binding (20). This response could be due to a direct fluorophore-ligand interaction, an agonist-induced conformational change associated with channel opening, or an agonist-induced conformational change that is unrelated to channel opening. A standard assumption we used in this study is that ligands that produce significantly different ΔF_{max} values produce different microenvironmental changes (16, 18, 24). In cases where this occurs, we discuss whether such changes may represent distinct conformational changes and, if so, whether these may be relevant to receptor activation. We also assume that if an agonist and an antagonist produce a similar ΔF_{max} then that microenvironmental change does not represent a conformational change essential for gating. While recognizing that different conformational changes may elicit similar ΔF responses, the most conservative interpretation is that a ΔF_{max} of defined direction and magnitude represents a unique conformational change.

If an agonist-mediated ΔF concentration response is right-shifted relative to the ΔI concentration response, then we infer that ΔF is unlikely to be reporting a conformational change essential for gating because at low agonist concentrations the channel can be activated without a ΔF response (18). It has previously been argued that if a ΔF concentration response is modestly left-shifted relative to the ΔI concentration response then ΔF may be reporting an agonist binding event (16). The rationale for this is that multiple bound agonists per receptor are required for complete receptor activation, whereas a single bound agonist per receptor should be sufficient to elicit a significant ΔF but not a significant ΔI. In the present study, we extend this interpretation to assume that such a ΔF may report either a direct steric agonist interaction or a local conformational change induced by the binding of a single agonist. We define "local" as a conformational change that may extend between subunits but does not propagate to the gate.

α1 Subunit Loop F—The GABA binding pocket is formed by β2 subunit loops A, B, and C (which form the principle or + side of the interface) and α1 subunit loops D, E, and F (which form the complementary or − side of the interface). Crystallography studies on acetylcholine-binding protein demonstrated that loop F distends when ligands bind to this site (13–15). However, functional studies have not reached consensus on whether such movements form an essential component of the gating mechanism (17).

In the present study, we identified an α1 subunit residue (α1-R186C) that, following labeling with MTS-R, produced a ΔF_{max} that was similar in magnitude for the full agonist, GABA; the low efficacy agonist, β-alanine; and the antagonist, gabazine. We also showed that at low agonist concentrations the ΔF signal was proportionately larger than the ΔI signal (Fig. 2, *B* and *C*). The most conservative explanation for all these results is that the attached label is either directly interacting with the bound ligands or, more likely, is reporting a local conformational change that occurs as a consequence of ligand binding. Given that both agonists and a structurally distinct antagonist produced identical ΔF_{max} values, such a conformational change is unlikely to be associated with channel gating or ligand recognition.

These results are generally consistent with those obtained previously at structurally related homomeric ρ1 GABA$_A$Rs and homomeric α1 GlyRs (16, 18, 19). α1-R186C aligns with S223C in the ρ1 GABA$_A$R subunit. A fluorescent label attached to ρ1-S233C produced a negative ΔF_{max} that was largest for GABA, smaller in magnitude for two partial agonists, and smaller again but still significant for an antagonist (16). However, pooling results from a range of labeled residues in the ρ1 GABA$_A$R loop F, there proved to be no correlation between agonist efficacy and the size of the corresponding ΔF_{max} throughout this domain (16, 19). A similar situation was observed at two labeled F loop sites in the α1 GlyR where agonists and an antagonist produced identical ΔF_{max} responses (18, 29). On the basis of all these results, it must be concluded that ΔF_{max} of a label attached to α1-R186C or corresponding residues in other Cys-loop receptors reports a local conformational change that is not part of the channel activation mechanism.

It has been reported that picrotoxin, which binds in the pore (43, 44), can affect ΔF responses of labels attached to ρ1 GABA$_A$R loop F residues (19). Although this demonstrates that perturbations of distant sites can allosterically affect loop F conformation (see also the next section), it does not necessarily imply that such conformational changes are involved in channel activation.

β2 Subunit Loop F—This domain is not part of the agonist binding pocket, and hence, ligand-mediated Δ*F* responses of labels attached to this domain must be allosterically mediated. In the present study, we investigated Δ*F* responses of MTS-TAMRA attached to β2-I180C in loop F. We demonstrated here that the GABA- and β-alanine-evoked ΔF_{max} values were identical to each other but that the gabazine-induced ΔF_{max} was significantly smaller. Moreover, at low concentrations of both GABA and β-alanine, the Δ*F* signal was proportionately larger than the Δ*I* signal (Fig. 3, *B* and ***C***). We also found that n_H values were decreased dramatically for Δ*F versus* Δ*I* concentration-response relationships. Together, these results are consistent with agonists and antagonists inducing distinct allosteric conformational changes in the β2 subunit loop F domain. However, our observations do not necessarily imply a role for the agonist-induced conformational change in receptor activation. Loop F is physically connected to loop C of the same subunit (4). Because the β2 subunit loop C is part of the agonist binding site, but loop F is not, changes in loop C conformation induced by ligand binding could produce conformational changes in loop F. We suggest that the conformational change induced in β2 subunit loop F is allosteric and was probably elicited by loop C of the same subunit "clasping" around the bound agonist (6). Although this interpretation has previously been invoked (17), it was made on the basis of data recorded in homomeric Cys-loop receptors where it was not possible to determine whether Δ*F* signals emanated from ligand-bound subunits, ligand-unbound subunits, or both.

γ2 Subunit Loop F—Loop F of the γ2 subunit does not contribute to the binding sites for GABA, β-alanine, or gabazine, although it does contribute to the high affinity benzodiazepine and DMCM binding sites (34, 45–49). On the basis of their significantly different ΔF_{max} values, our results indicate that GABA and β-alanine induce distinct allosteric conformational changes in this domain. In contrast, gabazine produced no detectable Δ*F*. The positive correlation between agonist efficacy and ΔF_{max} magnitude for all three ligands suggests that this conformational change may be associated with activation. This is reasonable as GABA does not bind to either interface involving the γ2 subunit and thus can only induce a conformation in it via a concerted allosteric conformational change.

A 10 μM concentration of diazepam applied to TMRM-tagged α1 β2 γ2-S195C GABA$_A$Rs produced a Δ*F* of 0.33%. Because a higher (100 μM) diazepam concentration produced no additional Δ*F* response and is insufficient to saturate the low affinity site (34), we conclude that the observed Δ*F* response represents the ΔF_{max} in response to diazepam binding to the high affinity site. We also found that a strongly inhibiting (10 μM) concentration of DMCM produced a ΔF_{max} response similar in magnitude to that elicited by diazepam. As the two ligands both bind at the α1-γ2 interface, we conclude that the ΔF_{max} signals a common conformational change in response to ligand occupation of this site.

There is evidence for a second high affinity benzodiazepine site located at the α4-β3 LBD interface. This is based largely on experiments on α4 β3 δ GABA$_A$Rs where it was shown that a δ subunit mutation increased diazepam binding to the α4-δ interface without affecting the already present Ro15-4513 binding site (50). Unfortunately, the pharmacological selectivity profile of this site is not known. The possible existence of such a site at the LBD α1-β2 interface would not affect the conclusions of this study as this site would still remain physically distinct from the GABA site at the β2-α1 subunit interface.

Summary Loop F—We demonstrated that ligand occupation of a β2-α1 interface GABA binding site can produce allosteric conformational changes to the β2 subunit loop F that faces the adjacent non-ligand-binding subunit interface. As loop F and loop C are physically connected by a short strand within a single subunit, the most likely explanation is that loop C closure around the bound ligand at one interface directly alters loop F conformation at the adjacent interface. As suggested previously (17), this provides a mechanism to explain how adjacent agonist binding sites can interact and thus provides a mechanism to explain cooperative activation in homomeric pentameric Cys-loop receptors (51). Of course, as heteromeric GABA$_A$Rs do not have adjacent GABA binding sites, this mechanism does not necessarily apply. We also found that high and low efficacy agonists and an antagonist induce identical loop F conformational changes in α1 subunits. This suggests that loop F conformational changes observed in GABA$_A$R and GlyR binding sites are not involved in ligand discrimination. However, because a labeled GABA$_A$R β2 subunit loop F residue responded differently to agonists and an antagonist, it is possible that loop C movements may mediate ligand discrimination and transmit these to loop F of the adjacent non-ligand-binding interface. Consistent with this, it has previously been concluded that loop C is involved in ligand discrimination on the basis of structural data (13–15) and VCF studies on the homomeric ρ1 GABA$_A$R and α1 GlyR (18, 30). Finally, mediated Δ*F* responses in the labeled γ2 subunit induced by GABA, β-alanine, and gabazine were likely to have been caused by concerted local conformational changes as this subunit does not bind these ligands.

α1 Subunit TM2-TM3 Domain—As this domain lies distant from the ligand binding sites, ligand-mediated Δ*F* responses observed in this domain must be mediated allosterically. The initial ΔF_{max} responses elicited by saturating concentrations of GABA and β-alanine at TMRM-tagged α1-N20′C β2 GABA$_A$Rs were indistinguishable from each other, whereas gabazine produced no detectable Δ*F*. This suggests a common agonist-mediated conformational change in this region. We do not know why Δ*F* responses declined dramatically with successive agonist applications. One possibility is that the fluorophore orientation was irreversibly altered by the first agonist application. Alternatively, the fluorophore could be irreversibly quenched by photoinduced electron transfer in the open state. Unfortunately, the inability to compare Δ*F* and Δ*I* agonist concentration-response relationships limited our ability to interpret the Δ*F* responses observed in this region. Nevertheless, as gabazine induced no Δ*F* response, the observed Δ*F* is consistent with a role in activation.

The TMRM-labeled α1-N20′C β2 GABA$_A$R also displayed an increased Δ*F* response following application of 100 μM diazepam. Dimeric α1 β2 GABA$_A$Rs contain only low affinity

diazepam sites that are thought to be located in the transmembrane region (34). We interpret this Δ*F* as a conformational change mediated following occupation of the low affinity site. Interestingly, incorporation of the γ2 subunit resulted in a Δ*F* that was reversed in magnitude. As this was activated by a low (10 μM) concentration of diazepam, we conclude that it occurred in response to occupation of the high affinity site α1-γ2 interface site. Thus, occupation of high and low affinity diazepam sites produces different conformational changes in the α1 subunit TM2-TM3 domain. This is the first evidence for different conformational changes mediated by different concentrations of diazepam.

β2 Subunit TM2-TM3 Domain—The MTS-R-labeled α1 β2-K24′C GABA$_A$R exhibited similar GABA- and β-alanine-mediated ΔF_{max} responses. Moreover, the respective GABA and β-alanine Δ*I* and Δ*F* concentration-response relationships overlapped closely (Fig. 6). These results suggest that GABA and β-alanine produce similar conformational changes in this domain that may be important for activation. This interpretation is strengthened by the observation that gabazine produced a Δ*F* response opposite in sign to that produced by the agonists. The reason this effect was not observed in a previous study (25) may have been due to the use of a different fluorophore and/or an insufficiently high gabazine concentration. Our result provides evidence for gabazine, supposedly a classical competitive antagonist, inducing conformational changes in the gating domain distant from its binding site. We note, however, that incorporation of the γ2 subunit abolished this Δ*F* response. It is unlikely this can be explained by a reduction in the number of labeled β2-K24′C subunits per receptor as incorporation of γ2 subunits would have only halved the number of β2-K24′C subunits but at the same time would have increased the number of uncross-linked β2-K24′C subunits available for labeling. Thus, the most likely explanation for the reduction in magnitude of the gabazine-mediated Δ*F* is a structural change imposed by the γ2 subunit.

Incorporation of γ2 subunits resulted in small increases in GABA and β-alanine Δ*F* EC_{50} values relative to the corresponding Δ*I* EC_{50} values. This provides further evidence for a structural change imposed by the γ2 subunit. Beyond this, however, it is difficult to interpret to this result. One possibility is that in the dimeric receptor the K24′C label is detecting conformational change associated with gating, but in the trimeric receptor, it may be detecting a conformational change unrelated to gating (28).

Cross-linking of Adjacent β2 Subunits—Several observations prompted us to conclude that adjacent β2 subunit residues dimerize efficiently via disulfide bonds between their respective K-24′C residues. First, current magnitude in α1 β2-K24′C GABA$_A$Rs was increased by a reducing agent and irreversibly reduced by an oxidizing agent. Second, Western blot analysis showed a dramatically increased dimer formation in α1 β2-K24′C GABA$_A$Rs relative to α1 β2 GABA$_A$Rs. Finally, incorporation of γ2 subunits, which prevents the formation of GABA$_A$Rs containing adjacent β2 subunits, also dramatically increased current magnitude. This rules out the possibility of dimer formation between non-adjacent β2-K24′C subunits. It is also unlikely that dimers may have formed between β2-K24′C and α1 or γ2 subunits due to the lack of nearby free cysteine groups on those subunits. β subunit dimerization has previously been reported to inhibit receptor activation in dimeric α1 β1-T6′C and α1 β2-E20′C GABA$_A$Rs and in trimeric α1 β1-E20′C γ2 GABA$_A$Rs (39, 40, 42). These studies concluded that either spontaneous β subunit movements, asymmetric movements of adjacent β subunits, or both were essential for channel activation. The present study demonstrates that dimerization of β subunits via residues extracellular to TM2 can also inhibit receptor activation. Cysteine α-carbon atoms must move to within a distance of 5–6 Å of each other to form a disulfide bond (52). Of course, this may represent a minimum distance reached at the limits of their respective mobility ranges and may be much less than their average separation. The secondary structure of the GABA$_A$R β subunit has not been unequivocally established. According to both the *Torpedo* nAChR structure (38) and substituted cysteine accessibility studies on both α1 β1 GABA$_A$Rs (53) and muscle nAChRs (54), the TM2 α-helical structure extends beyond 24′. In the nAChR structure, adjacent subunit 24′ α-carbons are located ~17 Å apart. On the other hand, the prokaryotic GLIC Cys-loop receptor structure shows the 24′ residue to be located in an unstructured loop that extends radially outward from the 19′ residue at the top of the TM2 α-helix (7, 8). In this model, adjacent subunit Lys-24′ α-carbons are located 23 Å apart. Our finding of a β2-K24′C cross-link therefore provides evidence for exceptionally large thermal motions in the 24′ region of β subunits. However, this result does not unequivocally favor one structural model over the other.

γ2 Subunit TM2-TM3 Domain—TMRM-tagged α1 β2 γ2-P23′C GABA$_A$Rs displayed identical GABA- and β-alanine-evoked ΔF_{max} values, whereas gabazine elicited no Δ*F* response. This pattern is similar to that observed in labeled TM2-TM3 residues in α1 and β2 subunits. It thus suggests that GABA and β-alanine produce similar conformational changes in this region, whereas gabazine does not. This is consistent with a role for this conformational change in receptor activation. We also observed a small diazepam-induced Δ*F*, suggesting that γ2-P23′C may be reporting a conformational change associated with diazepam modulation.

Summary TM2-TM3 Domain—Gabazine, a putative competitive antagonist, produced TM2-TM3 domain conformational changes that were markedly different from those produced by agonists. As β-alanine and GABA produced identical ΔF_{max} responses at labeled TM2-TM3 residues in all three subunits, it appears that conformational changes were similar for the two agonists. Together, these results suggest that the agonist-mediated Δ*F* responses may be reporting conformational changes involved with gating. The detection of conformational changes in the TM2-TM3 domains of all three subunits implies cooperativity at this point in the activation "conformational wave" (36). Although we were unable to detect robust diazepam- or DMCM-mediated Δ*F* responses at most tested TM2-TM3 sites, our results do indicate that occupation of the high and low affinity diazepam binding sites results in strikingly different conformational changes in the

α1 subunit TM2-TM3 domain. Finally, we were surprised to discover that adjacent β subunits could be cross-linked via β2-K24′C disulfide bonds. In the nAChR and GLIC receptor structures, adjacent 24′ α-carbons are separated by 19 and 23 Å, respectively. As disulfide bond formation requires a cysteine α-carbon separation of 5–6 Å, our results demonstrate surprisingly large thermal motions in this region that, when prevented by disulfide formation, can inhibit gating.

Conclusions—This study provides evidence for both ligand- and subunit-specific conformational changes in both loop F and the TM2-TM3 linker. We provide no evidence that the loop F conformational changes are important for channel gating. However, conformational changes in the loop F domains of β2 and γ2 subunits are allosterically induced by ligands binding to β2-α1 interface binding sites. We also demonstrate that gabazine, a putative competitive antagonist, induces conformational changes in the TM2-TM3 domain. Finally, we demonstrate that TM2-TM3 loop 24′ residues from adjacent β2 subunits can move into close physical proximity to each other, indicating unexpected conformational freedom in this crucial part of the gating machinery. Together, this information provides new insights into the activation mechanisms of Cys-loop receptors.

REFERENCES

1. Sieghart, W., and Sperk, G. (2002) *Curr. Top. Med. Chem.* **2,** 795–816
2. Karlin, A. (2002) *Nat. Rev. Neurosci.* **3,** 102–114
3. Miller, P. S., and Smart, T. G. (2010) *Trends Pharmacol. Sci.* **31,** 161–174
4. Brejc, K., van Dijk, W. J., Klaassen, R. V., Schuurmans, M., van Der Oost, J., Smit, A. B., and Sixma, T. K. (2001) *Nature* **411,** 269–276
5. Unwin, N. (2005) *J. Mol. Biol.* **346,** 967–989
6. Unwin, N., Miyazawa, A., Li, J., and Fujiyoshi, Y. (2002) *J. Mol. Biol.* **319,** 1165–1176
7. Bocquet, N., Nury, H., Baaden, M., Le Poupon, C., Changeux, J. P., Delarue, M., and Corringer, P. J. (2009) *Nature* **457,** 111–114
8. Hilf, R. J., and Dutzler, R. (2009) *Nature* **457,** 115–118
9. Taly, A., Delarue, M., Grutter, T., Nilges, M., Le Novère, N., Corringer, P. J., and Changeux, J. P. (2005) *Biophys. J.* **88,** 3954–3965
10. Auerbach, A. (2010) *J. Physiol.* **588,** 573–586
11. Cederholm, J. M., Schofield, P. R., and Lewis, T. M. (2009) *Eur. Biophys. J.* **39,** 37–49
12. Sine, S. M., and Engel, A. G. (2006) *Nature* **440,** 448–455
13. Bourne, Y., Talley, T. T., Hansen, S. B., Taylor, P., and Marchot, P. (2005) *EMBO J.* **24,** 1512–1522
14. Celie, P. H., Kasheverov, I. E., Mordvintsev, D. Y., Hogg, R. C., van Nierop, P., van Elk, R., van Rossum-Fikkert, S. E., Zhmak, M. N., Bertrand, D., Tsetlin, V., Sixma, T. K., and Smit, A. B. (2005) *Nat. Struct. Mol. Biol.* **12,** 582–588
15. Hansen, S. B., Sulzenbacher, G., Huxford, T., Marchot, P., Taylor, P., and Bourne, Y. (2005) *EMBO J.* **24,** 3635–3646
16. Khatri, A., Sedelnikova, A., and Weiss, D. S. (2009) *Biophys. J.* **96,** 45–55
17. Khatri, A., and Weiss, D. S. (2010) *J. Physiol.* **588,** 59–66
18. Pless, S. A., and Lynch, J. W. (2009) *J. Biol. Chem.* **284,** 15847–15856
19. Zhang, J., Xue, F., and Chang, Y. (2009) *J. Physiol.* **587,** 139–153
20. Gandhi, C. S., and Isacoff, E. Y. (2005) *Trends Neurosci.* **28,** 472–479
21. Mannuzzu, L. M., Moronne, M. M., and Isacoff, E. Y. (1996) *Science* **271,** 213–216
22. Dahan, D. S., Dibas, M. I., Petersson, E. J., Auyeung, V. C., Chanda, B., Bezanilla, F., Dougherty, D. A., and Lester, H. A. (2004) *Proc. Natl. Acad. Sci. U.S.A.* **101,** 10195–10200
23. Mourot, A., Bamberg, E., and Rettinger, J. (2008) *J. Neurochem.* **105,** 413–424
24. Muroi, Y., Czajkowski, C., and Jackson, M. B. (2006) *Biochemistry* **45,** 7013–7022
25. Muroi, Y., Theusch, C. M., Czajkowski, C., and Jackson, M. B. (2009) *Biophys. J.* **96,** 499–509
26. Pless, S. A., Dibas, M. I., Lester, H. A., and Lynch, J. W. (2007) *J. Biol. Chem.* **282,** 36057–36067
27. Pless, S. A., and Lynch, J. W. (2008) *Clin. Exp. Pharmacol. Physiol.* **35,** 1137–1142
28. Pless, S. A., and Lynch, J. W. (2009) *J. Neurochem.* **108,** 1585–1594
29. Pless, S. A., and Lynch, J. W. (2009) *J. Biol. Chem.* **284,** 27370–27376
30. Chang, Y., and Weiss, D. S. (2002) *Nat. Neurosci.* **5,** 1163–1168
31. Cromer, B. A., Morton, C. J., and Parker, M. W. (2002) *Trends Biochem. Sci.* **27,** 280–287
32. Jones, M. V., Sahara, Y., Dzubay, J. A., and Westbrook, G. L. (1998) *J. Neurosci.* **18,** 8590–8604
33. Ueno, S., Bracamontes, J., Zorumski, C., Weiss, D. S., and Steinbach, J. H. (1997) *J. Neurosci.* **17,** 625–634
34. Walters, R. J., Hadley, S. H., Morris, K. D., and Amin, J. (2000) *Nat. Neurosci.* **3,** 1274–1281
35. Padgett, C. L., and Lummis, S. C. (2008) *J. Biol. Chem.* **283,** 2702–2708
36. Grosman, C., Zhou, M., and Auerbach, A. (2000) *Nature* **403,** 773–776
37. Lynch, J. W., Rajendra, S., Pierce, K. D., Handford, C. A., Barry, P. H., and Schofield, P. R. (1997) *EMBO J.* **16,** 110–120
38. Miyazawa, A., Fujiyoshi, Y., and Unwin, N. (2003) *Nature* **423,** 949–955
39. Horenstein, J., Riegelhaupt, P., and Akabas, M. H. (2005) *J. Biol. Chem.* **280,** 1573–1581
40. Horenstein, J., Wagner, D. A., Czajkowski, C., and Akabas, M. H. (2001) *Nat. Neurosci.* **4,** 477–485
41. Shan, Q., Haddrill, J. L., and Lynch, J. W. (2002) *J. Biol. Chem.* **277,** 44845–44853
42. Yang, Z., Webb, T. I., and Lynch, J. W. (2007) *J. Biol. Chem.* **282,** 16803–16810
43. Sedelnikova, A., Smith, C. D., Zakharkin, S. O., Davis, D., Weiss, D. S., and Chang, Y. (2005) *J. Biol. Chem.* **280,** 1535–1542
44. Yang, Z., Cromer, B. A., Harvey, R. J., Parker, M. W., and Lynch, J. W. (2007) *J. Neurochem.* **103,** 580–589
45. Buhr, A., Schaerer, M. T., Baur, R., and Sigel, E. (1997) *Mol. Pharmacol.* **52,** 676–682
46. Casula, M. A., Bromidge, F. A., Pillai, G. V., Wingrove, P. B., Martin, K., Maubach, K., Seabrook, G. R., Whiting, P. J., and Hadingham, K. L. (2001) *J. Neurochem.* **77,** 445–451
47. Davies, M., Bateson, A. N., and Dunn, S. M. (1998) *J. Neurochem.* **70,** 2188–2194
48. Hanson, S. M., and Czajkowski, C. (2008) *J. Neurosci.* **28,** 3490–3499
49. Wingrove, P. B., Thompson, S. A., Wafford, K. A., and Whiting, P. J. (1997) *Mol. Pharmacol.* **52,** 874–881
50. Meera, P., Olsen, R. W., Otis, T. S., and Wallner, M. (2010) *Mol. Pharmacol.* **78,** 918–924
51. Changeux, J. P., and Edelstein, S. J. (2005) *Science* **308,** 1424–1428
52. Careaga, C. L., and Falke, J. J. (1992) *J. Mol. Biol.* **226,** 1219–1235
53. Bera, A. K., Chatav, M., and Akabas, M. H. (2002) *J. Biol. Chem.* **277,** 43002–43010
54. Wiltfong, R. E., and Jansen, M. (2009) *J. Neurosci.* **29,** 1626–1635